

Measurement of the Nucleon Strange-Antistrange Asymmetry at Next-to-Leading Order in QCD from NuTeV Dimuon Data

D. Mason, J. Brau, R. B. Drucker, and R. Frey
University of Oregon, Eugene, Oregon, USA

P. Spentzouris, J. Conrad, B. T. Fleming, J. Formaggio, J. H. Kim, S. Koutsoliotas, C. McNulty, A. Romosan, M. H. Shaevitz, E. G. Stern, A. Vaitaitis, and E. D. Zimmerman
Columbia University, New York, New York 10027, USA

R. A. Johnson, N. Suwonjandee, and M. Vakili
University of Cincinnati, Cincinnati, Ohio 45221, USA

R. H. Bernstein, L. Bugel, M. J. Lamm, W. Marsh, P. Nienaber, N. Tobien, and J. Yu
Fermi National Accelerator Laboratory, Batavia, Illinois 60510, USA

T. Adams, A. Alton, T. Bolton, J. Goldman, and M. Goncharov
Kansas State University, Manhattan, Kansas 66506, USA

L. de Barbaro, D. Buchholz, H. Schellman, and G. P. Zeller
Northwestern University, Evanston, Illinois 60208, USA

S. Boyd, J. McDonald, D. Naples, V. Radescu, and M. Tzanov
Department of Physics, University of Pittsburgh, Pennsylvania 15260, USA

S. Avvakumov, P. de Barbaro, A. Bodek, H. Budd, D. A. Harris, K. S. McFarland, W. K. Sakumoto, and U. K. Yang
University of Rochester, Rochester, New York 14627, USA
(Received 25 March 2007; published 7 November 2007)

We present a new measurement of the difference between the nucleon strange and antistrange quark distributions from dimuon events recorded by the NuTeV experiment at Fermilab. This analysis is the first to use a complete next to leading order QCD description of charm production from neutrino scattering. Dimuon events in neutrino deep inelastic scattering allow direct and independent study of the strange and antistrange content of the nucleon. We find a positive strange asymmetry with a significance of 1.6σ . We also report a new measurement of the charm mass.

DOI: [10.1103/PhysRevLett.99.192001](https://doi.org/10.1103/PhysRevLett.99.192001)

PACS numbers: 14.20.Dh, 12.38.Qk, 13.15.+g, 14.65.Dw

Introduction.—The simple picture of a perturbatively generated nucleon quark sea through virtual $q\bar{q}$ pair production implies equal strange and antistrange seas. The nucleon carries no net strangeness, so the integrated difference between the strange and antistrange parton distributions, $\int_0^1 [s(x) - \bar{s}(x)] dx$, where x is the parton momentum fraction, must be zero. There is however no such restriction on the momentum distributions, $xs(x)$ and $x\bar{s}(x)$. Indeed, several theoretical models have been proposed which predict an asymmetry, such that $S^- \equiv \int_0^1 [xs(x) - x\bar{s}(x)] dx$ is nonzero [1–5]. Until now, there has been little experimental constraint on such an asymmetry, leading to much phenomenological speculation [6–10], most recently in the context of the NuTeV $\sin^2\theta_W$ measurement [11], found to be approximately 3σ above the world average. An asymmetry in the strange and antistrange seas, assumed to be zero in Ref. [11], would affect the measured value of $\sin^2\theta_W$. In order to bring the NuTeV measurement into

agreement with the value predicted by standard electro-weak theory [12], S^- would need to be of order $\sim +0.007$ [13,14], assuming an asymmetry in an x range between 0.02 and 0.2.

The strange and antistrange seas are directly accessible through the measurement and study of dimuon events in neutrino and antineutrino deep inelastic scattering (DIS) [15]. These events occur in charm production from charged current (CC) interactions with strange (or through Cabibbo suppressed, down) quarks in the nucleon. Neutrino (antineutrino) interactions generate charmed (anticharmed) hadrons from the strange (antistrange) sea. Approximately 10% of the time, the charmed hadrons decay semi-muonically, resulting in a final state with two oppositely charged muons and a hadronic shower from the nucleon breakup and charm decay. The second muon provides a clear signal by which to distinguish these events from other CC interactions.

The NuTeV experiment, executed during Fermilab's 1996-97 fixed target run, recorded 5163 (1380) dimuon events in neutrino (antineutrino) running mode with reconstructed neutrino energies ranging from 20–400 GeV. The NuTeV detector was continuously calibrated throughout the data run with muon, electron, and hadron calibration beams, significantly reducing uncertainties in detector response [16]. NuTeV's beamline was constructed to select ν_μ or $\bar{\nu}_\mu$ beams with very high purity [17,18], with more than 99% of CC events resulting from the selected ν or $\bar{\nu}$ type. This *a priori* knowledge of the beam mode allows precise separation of neutrino and antineutrino produced dimuons by muon sign, which in turn provides the ability to independently extract the strange and antistrange seas.

The large size of the gluon distribution requires study of the strange sea and charm production be performed at next to leading order (NLO) in QCD in order to have meaning beyond the context of neutrino-nucleon scattering. The measurement presented here represents the first extraction of the strange and antistrange sea distributions with a complete NLO QCD model differential in all variables required to describe event acceptance [19].

Analysis method.—The NuTeV dimuon data have been presented in the form of a model independent forward dimuon cross section table [20–22]. This table is defined to be the cross section of dimuon events from charm production in iron such that the muon from the semileptonic charm decay has energy greater than 5 GeV (hence “forward”). The table is extracted at the weighted center of 3 bins in neutrino energy (E_ν), 3 in the inelasticity ($y \equiv \frac{E_{\text{Had}}}{E_\nu}$, where E_{Had} is the hadronic shower energy), and 5 in Bjorken x , for both neutrino and antineutrino dimuon data. The table is extracted with a method insensitive to physics model assumptions and has been corrected for detector smearing effects and backgrounds.

The strange sea is determined by performing a χ^2 fit of the acceptance corrected dimuon cross section to the table data. The following expression illustrates the components making up this fit:

$$\frac{d\sigma_{\text{charm}}}{dxdy} B_c \otimes \mathcal{N} \otimes \mathcal{A} \Leftarrow \boxed{\text{fit}} \Rightarrow \frac{d\sigma_{2\mu}}{dxdy} \quad (1)$$

Model parameters on the left side of $\Leftarrow \boxed{\text{fit}} \Rightarrow$ are varied to find the best χ^2 to the cross section table values, $\frac{d\sigma_{2\mu}}{dxdy} \cdot \frac{d\sigma_{\text{charm}}}{dxdy}$ is the NLO neutrino charm production cross section [23], dependent on the strange-antistrange sea and charm mass. The strange and antistrange seas are varied in the fit. The charm mass is constrained to the Particle Data Group value of 1.20 ± 0.10 [12]. B_c is the charm semileptonic branching ratio, which is an average over all produced charmed hadrons. A value of 0.099 ± 0.012 , from Fermilab E-531 data [24], is used. \mathcal{N} is the correction for nuclear effects, dependent on atomic number, struck quark flavor, x and scale Q^2 [25]. \mathcal{N} is applied to the individual parton

distribution functions (pdfs), which are in turn convolved within the charm cross section. \mathcal{A} is a kinematic acceptance correction which accounts for the 5 GeV cut on the energy of the charm decay muon. \mathcal{A} depends on E_ν , y , x , as well as charm fragmentation and charm mass.

A Monte Carlo simulation of dimuon events employing the DISCO [19] charm cross section model was used to calculate \mathcal{A} in each cross section bin. DISCO is an NLO cross section code which is differential in x , y , fragmentation momentum fraction z and charm transverse momentum, through the rapidity variable $\eta_c \equiv \frac{1}{2} \log \frac{E_c + p_{\text{cl}}}{E_c - p_{\text{cl}}}$. For each table bin, \mathcal{A} is determined by simulating dimuon events and finding the ratio of those with charm decay muon energy greater than 5 GeV over a grid of 20 z and 40 η_c bins weighted by $\frac{d\sigma_{\text{charm}}}{dxdydzd\eta_c}$. Charm fragmentation is described by the Collins-Spiller parametrization [26] with an ϵ_{C-S} value of 0.6 ± 0.3 , obtained by direct comparisons to NuTeV data.

Fits are based on the CTEQ6M pdf set [27], and a modified version of the EVLCTEQ evolution package which accommodates $s(x) \neq \bar{s}(x)$ [28]. The strange sea is described using the following parametrization [29]:

$$s^+(x) = \kappa^+ (1-x)^{\alpha^+} x^{\gamma^+} [\bar{u}(x) + \bar{d}(x)] \quad (2)$$

$$s^-(x) = s^+(x) \tanh \left[\kappa^- (1-x)^{\alpha^-} x^{\gamma^-} \left(1 - \frac{x}{x_0} \right) \right] \quad (3)$$

$$s = \frac{s^+ + s^-}{2} \bar{s} = \frac{s^+ - s^-}{2} \quad (4)$$

with $s^+(x)$ and $s^-(x)$ defined at an initial scale of $Q_0 = 1.3$ GeV, and evolved to a scale of $Q^2 + m_c^2$ for each of the cross section table bins. Six fit parameters, κ^+ , α^+ , γ^+ , κ^- , α^- , and γ^- describe the overall level and shape of the strange and antistrange seas. The flavor sum rule is enforced by finding the crossing point x_0 of s^- such that $\int_0^1 s^-(x) dx$ is zero. The nonstrange pdfs are held constant and treated as external constraints. The total momentum sum rule is maintained by rescaling the size of the gluon distribution to balance any increase or decrease in the size of xs^+ . Through the course of a typical fit, it is found that this rescaled gluon sea never deviates beyond a fraction of a percent from the CTEQ gluon sea (i.e., of order of a few percent of the uncertainty on the gluon sea).

Results.—Figures 1 and 2 show the fitted, acceptance corrected dimuon cross section along with the dimuon cross section data. A good fit with a χ^2 of 38.2 for 37.8 effective DOF is achieved. The overall size of the strange and antistrange seas is typically expressed as $\eta \equiv \frac{S^+}{U+D}$, where S^+ , U , and D are the summed analogues of S^- for strange, up and down, respectively. A value of $\eta = 0.061 \pm 0.001(\text{stat}) \pm 0.006(\text{syst})_{-0.012}^{+0.014}(\text{external})$ is obtained. The “external” error refers to the contribution due to the uncertainties on external measurements. If left

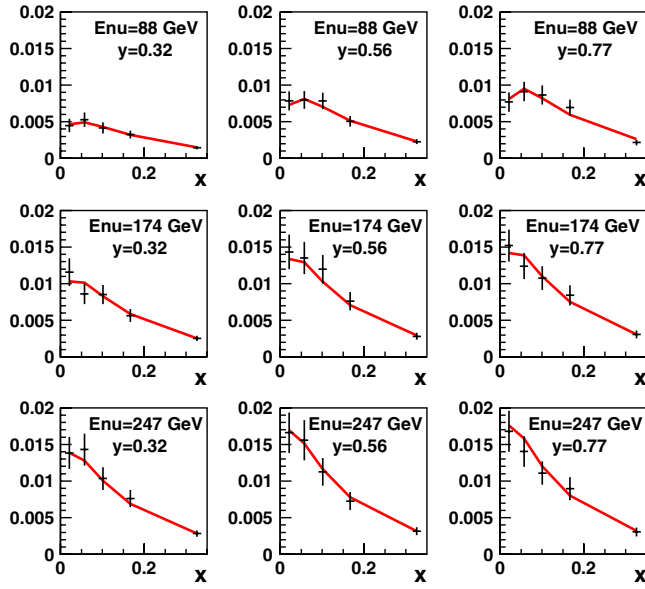


FIG. 1 (color online). ν forward dimuon cross section (points) and fit (curve) plotted vs x for each E_ν and y bin. The vertical scale is cross section multiplied by $\frac{\pi}{G_F^2 M E_\nu}$.

to vary in the fits, a charm mass of $1.41 \pm 0.10(\text{stat}) \pm 0.08(\text{syst})_{-0.08}^{+0.17}(\text{external})$ GeV is obtained.

Figure 3 shows the shape of $xs^-(x)$ resulting from the fit, with the outer error band indicating the combined error on the measurement. We find that $xs^-(x)$ tends positive, such that S^- is $0.00196 \pm 0.00046(\text{stat}) \pm 0.00045(\text{syst})_{-0.00107}^{+0.00148}(\text{external})$. The strange sea param-

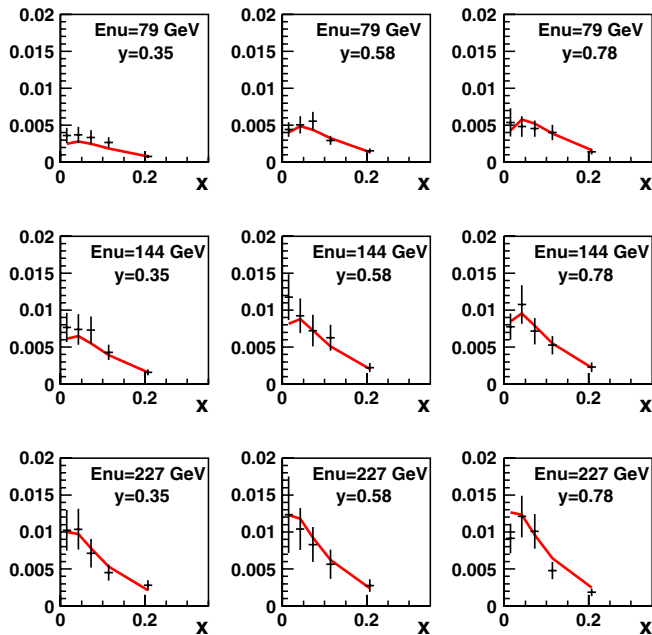


FIG. 2 (color online). $\bar{\nu}$ forward dimuon cross section (points) and fit (curve) plotted vs x for each E_ν and y bin. The vertical scale is cross section multiplied by $\frac{\pi}{G_F^2 M E_\nu}$.

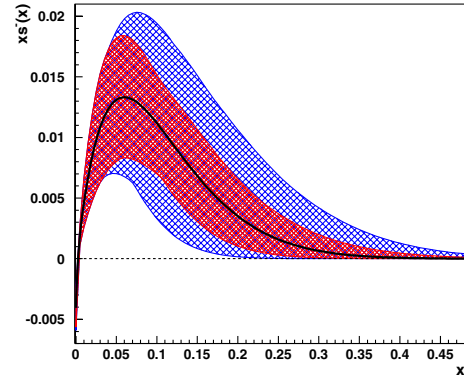


FIG. 3 (color online). $xs^-(x)$ vs x at $Q^2 = 16 \text{ GeV}^2$. Outer band is combined errors; inner band is without B_c uncertainty.

eters of the best fit are $\kappa^+ = 0.58$, $\alpha^+ = 1.40$, $\gamma^+ = 0.098$, $\kappa^- = -0.0094$, $\alpha^- = 6.59$, $\gamma^- = 0.0040$.

Table I separates out the individual contributions to the uncertainties. The dominant contribution is the large uncertainty in the average semileptonic branching ratio B_c , which is strongly anticorrelated with S^- . The inner error band in Fig. 3 shows the total S^- uncertainty without the B_c error.

TABLE I. Contributions to the error in S^- . Where significantly asymmetric, + and - contributions are shown. The systematic errors from the table extraction [20–22] are shown in the upper section of the table. The errors due to external measurement uncertainties are in the lower section. The nuclear correction uncertainty was estimated by comparing the difference between the de Florian [25] and Hirai [30] models. The Kulagin-Petti nuclear correction model [31], which predicts different nuclear effects between ν and $\bar{\nu}$ interactions at low x , was also studied, and the resulting change in the asymmetry was found to be well within this systematic.

0.00196	central value
± 0.00046	statistics
± 0.00034	$\nu \pi - K$ model
± 0.00025	$\bar{\nu} \pi - K$ model
± 0.00004	spectrometer momentum scale (1%)
± 0.00008	hadron energy scale (0.5%)
± 0.00005	R_L in table model (20%)
± 0.00001	table extraction MC statistics
± 0.00012	decay μ range out energy (2.5%)
± 0.00005	$\nu, \bar{\nu}$ relative normalization
± 0.00006	strange sea parametrization
± 0.00045	total systematics
± 0.00002	$\Delta m_c = 0.10$
$+0.00017 - 0.00026$	$\Delta \epsilon_{C-S} = 0.3$
$+0.00135 - 0.00086$	$\Delta B_c = 0.012$
± 0.00046	CTEQ6 pdf uncertainties
± 0.00038	Nuclear corrections
$+0.00148 - 0.00107$	total external measurement

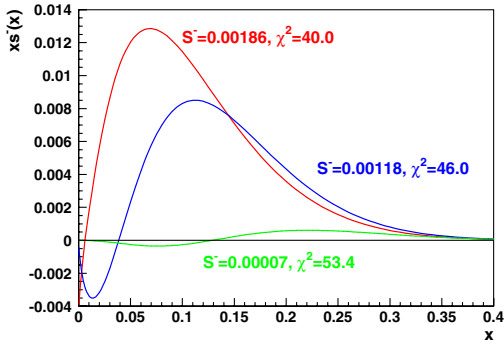


FIG. 4 (color online). xs^- for x_0 of 0.01, 0.05, and 0.15. χ^2 's are labeled for an effective DOF of 38.8.

The data prefer an asymmetry which satisfies the flavor sum rule by forcing $s^-(x)$ to spike negative below an x_0 of 0.004, where it is unconstrained by NuTeV data. If one chooses to fix the crossing point at higher values of x_0 , as suggested by some theoretical models, one finds the asymmetry shrinks with increasing x_0 at the expense of χ^2 . Figure 4 shows the results of three fits with fixed x_0 . The fits enforce the flavor sum rule by allowing γ^- to vary so that $\int_0^1 s^-(x)dx = 0$. As the crossing point reaches $x_0 = 0.15$, the asymmetry virtually disappears; however, the χ^2 grows to 53.4/38.8 DOF.

An alternate fit using a more traditional parametrization,

$$s(x, Q_0) = \kappa(1-x)^\alpha \left[\frac{\bar{u}(x, Q_0) + \bar{d}(x, Q_0)}{2} \right] \quad (5)$$

(and similar for $\bar{s}(x, Q_0)$), was tried, where the neutrino and antineutrino tables were treated as independent data samples with the same m_c , ϵ_{C-S} , and B_c . This fit produced an asymmetry of $0.00203 \pm 0.00056(\text{stat}) \pm 0.00055(\text{syst})_{-0.00109}^{+0.00150}(\text{external})$.

Conclusion.—We have presented the first measurement, using a complete NLO QCD treatment, of the asymmetry between the strange and antistrange quark distributions from neutrino DIS dimuon production, taking full advantage of NuTeV's highly pure ν and $\bar{\nu}$ beams. The overall level of the asymmetry tends positive, with a momentum weighted integral of $S^- = 0.00196 \pm 0.00046(\text{stat}) \pm 0.00045(\text{syst})_{-0.00107}^{+0.00148}(\text{external})$. The uncertainty is dominated by the large uncertainty on B_c and could be improved with better measurements of B_c for $E_\nu > 20$ GeV. The strange flavor sum rule prefers to be satisfied with a large negative spike at extremely low x . As the location where $s^-(x)$ crosses zero is fixed at higher values of x , the asymmetry shrinks, but at the expense of higher χ^2 . An alternate parametrization allowing violation of the flavor sum rule was tried with similar results. Taken by itself, the strange asymmetry is insufficient to explain the difference between the NuTeV $\sin^2\theta_W$ measurement and the world average. The charm mass was also measured, with a value of $1.41 \pm 0.10(\text{stat}) \pm 0.08(\text{syst})_{-0.08}^{+0.17}(\text{external})$ GeV.

The authors wish to thank J. Amundson, S. Kretzer, F. Olness, W.K. Tung, R. Sassot, T. Signal, and D. Soper for code and many helpful discussions.

-
- [1] A. I. Signal and A. W. Thomas, Report No. ADP-87-54-T471987, 1987 (unpublished).
 - [2] M. Burkardt and B. J. Warr, Phys. Rev. D **45**, 958 (1992).
 - [3] S. J. Brodsky and B. Q. Ma, Phys. Lett. B **381**, 317 (1996).
 - [4] G. Rodrigo, S. Catani, D. de Florian, and W. Vogelsang, Nucl. Phys. B, Proc. Suppl. **135**, 188 (2004).
 - [5] J. Alwall and G. Ingelman, Phys. Rev. D **71**, 094015 (2005).
 - [6] S. Davidson, S. Forte, P. Gambino, N. Rius, and A. Strumia, J. High Energy Phys. 02 (2002) 037.
 - [7] S. Kretzer, F. Olness, J. Pumplin, D. Stump, W. K. Tung, and M. H. Reno, Phys. Rev. Lett. **93**, 041802 (2004).
 - [8] F. G. Cao and A. I. Signal, Phys. Lett. B **559**, 229 (2003).
 - [9] J. Alwall and G. Ingelman, Phys. Rev. D **70**, 111505(R) (2004).
 - [10] Y. Ding, R. G. Xu, and B. Q. Ma, Phys. Lett. B **607**, 101 (2005).
 - [11] G. P. Zeller *et al.* (NuTeV Collaboration), Phys. Rev. Lett. **88**, 091802 (2002); (**90**), 239902(E) (2003).
 - [12] S. Eidelman *et al.* (Particle Data Group), Phys. Lett. B **592**, 1 (2004).
 - [13] G. P. Zeller *et al.* (NuTeV Collaboration), Phys. Rev. D **65**, 111103 (2002); (**67**), 119902(E) (2003).
 - [14] K. S. McFarland and S. O. Moch, arXiv:hep-ph/0306052.
 - [15] J. M. Conrad, M. H. Shaevitz, and T. Bolton, Rev. Mod. Phys. **70**, 1341 (1998).
 - [16] D. A. Harris and J. Yu *et al.* (NuTeV Collaboration), Nucl. Instrum. Methods Phys. Res., Sect. A **447**, 377 (2000).
 - [17] A. Alton *et al.* (NuTeV Collaboration), Phys. Rev. D **64**, 012002 (2001).
 - [18] R. Bernstein (NuTeV Collaboration), Fermilab Report No. FERMILAB-TM-1884, 1994 (unpublished).
 - [19] S. Kretzer, D. Mason, and F. Olness, Phys. Rev. D **65**, 074010 (2002).
 - [20] M. Goncharov *et al.* (NuTeV Collaboration), Phys. Rev. D **64**, 112006 (2001).
 - [21] D. Mason (NuTeV Collaboration), AIP Conf. Proc. No. 792 (AIP, Madison, WI, 2005), pp. 851-854.
 - [22] D. Mason, Ph.D. thesis, University of Oregon, 2006.
 - [23] M. Gluck, S. Kretzer, and E. Reya, Phys. Lett. B **380**, 171 (1996); **405**, 391(E) (1997).
 - [24] T. Bolton, arXiv:hep-ex/9708014.
 - [25] D. de Florian and R. Sassot, Phys. Rev. D **69**, 074028 (2004).
 - [26] P. D. B. Collins and T. P. Spiller, J. Phys. G **11**, 1289 (1985).
 - [27] J. Pumplin, D. R. Stump, J. Huston, H. L. Lai, P. Nadolsky, and W. K. Tung, J. High Energy Phys. 07 (2002) 012.
 - [28] W. K. Tung (private communication).
 - [29] F. Olness *et al.*, Eur. Phys. J. C **40**, 145 (2005).
 - [30] M. Hirai, S. Kumano, and T. H. Nagai, Phys. Rev. C **70**, 044905 (2004).
 - [31] S. A. Kulagin and R. Petti, arXiv:hep-ph/0703033 [Phys. Rev. D (to be published)].